Received: 1 February 2022 | Revised: 23 April 2022 | Accepted: 29 April 2022

DOI: 10.1096/fj.202200189RR

THE FASEB JOURNAL

RESEARCH ARTICLE

CTRP11 contributes modestly to systemic metabolism and energy balance

Dylan C. Sarver[1,2] | **Cheng Xu**[1,2] | **Dana Carreno**[1,2] | **Alexander Arking**[1,2] | **Chantelle E. Terrillion**[3] | **Susan Aja**[2,4] | **G. William Wong**[1,2]

[1]Department of Physiology, Johns Hopkins University School of Medicine, Baltimore, Maryland, USA

[2]Center for Metabolism and Obesity Research, Johns Hopkins University School of Medicine, Baltimore, Maryland, USA

[3]Department of Psychiatry and Behavioral Sciences, Johns Hopkins University School of Medicine, Baltimore, Maryland, USA

[4]Department of Neuroscience, Johns Hopkins University School of Medicine, Baltimore, Maryland, USA

Correspondence
G. William Wong, Department of Physiology, Johns Hopkins University School of Medicine, Baltimore, MD 21205, USA.
Email: gwwong@jhmi.edu

Funding information
HHS | NIH | National Institute of Diabetes and Digestive and Kidney Diseases (NIDDK), Grant/Award Number: DK084171

Abstract

C1q/TNF-related proteins (CTRP1-15) constitute a conserved group of secreted proteins of the C1q family with diverse functions. In vitro studies have shown that CTRP11/C1QL4 can inhibit adipogenesis, antagonize myoblast fusion, and promote testosterone synthesis and secretion. Whether CTRP11 is required for these processes in vivo remains unknown. Here, we show that knockout (KO) mice lacking CTRP11 have normal skeletal muscle mass and function, and testosterone level, suggesting that CTRP11 is dispensable for skeletal muscle development and testosterone production. We focused our analysis on whether this nutrient-responsive secreted protein plays a role in controlling sugar and fat metabolism. At baseline when mice are fed a standard chow, CTRP11 deficiency affects metabolic parameters in a sexually dimorphic manner. Only *Ctrp11*-KO female mice have significantly higher fasting serum ketones and reduced physical activity. In the refeeding phase following food withdrawal, *Ctrp11*-KO female mice have reduced food intake and increased metabolic rate and energy expenditure, highlighting CTRP11's role in fasting–refeeding response. When challenged with a high-fat diet to induce obesity and metabolic dysfunction, CTRP11 deficiency modestly exacerbates obesity-induced glucose intolerance, with more pronounced effects seen in *Ctrp11*-KO male mice. Switching to a low-fat diet after obesity induction results in greater fat loss in wild type relative to KO male mice, suggesting impaired response to obesity reversal and reduced metabolic flexibility in the absence of CTRP11. Collectively, our data provide genetic evidence for novel sex-dependent metabolic regulation by CTRP11, but note the overall modest contribution of CTRP11 to systemic energy homeostasis.

KEYWORDS
C1QL4, C1QTNF11, metabolism, obesity reversal, secreted hormone

ABBREVIATIONS: CTRP, C1q/TNF-related protein; EE, energy expenditure; gWAT, gonadal white adipose tissue; HFD, high-fat diet; i.p., intraperitoneally; iWAT, inguinal white adipose tissue; KO, knockout; LFD, low-fat diet; NEFA, non-esterified free fatty acids; RER, respiratory exchange ratio; TG, triglyceride; WT, wild type.

1 | INTRODUCTION

The discovery of immune complement C1q[1] has led to the subsequent identification of other related proteins, all of which possess the signature C-terminal globular domain homologous to C1q in sequence and structure.[2,3] This highly conserved and functionally diverse group of secreted proteins, encoded by >30 unique genes, collectively made up the C1q family.[4,5] Within this family, there is a subgroup of 15 proteins referred to as the C1q/TNF-related proteins (CTRP1-15),[6] which we have initially identified based on shared sequence homology to the insulin-sensitizing hormone, adiponectin.[7,8] Multiple approaches—involving recombinant protein infusion, transgenic overexpression, and knockout mouse models—have provided critical in vivo evidence for CTRPs in regulating diverse aspects of glucose and lipid metabolism,[9–26] obesity-linked low-grade inflammation,[10,27] as well as other diverse functions in the heart and vasculature,[28–34] kidney,[35–37] muscle and tendon,[38,39] bone,[40] immune system,[41–44] and the central nervous system.[45–48]

Of the CTRP family members, the physiological function of CTRP11/C1QL4 still remains largely unknown. We identified CTRP11 based on its shared sequence homology to other related CTRP family members.[49] *CTRP11* is robustly expressed by adipose tissue in both human and mice, and within the adipose tissue, CTRP11 is predominantly derived from cells of the stromal vascular compartment.[49] We have shown that CTRP11 overexpression or treatment with recombinant CTRP11 potently suppresses 3T3-L1 adipocyte differentiation in vitro, suggesting that CTRP11 could function as an endogenous paracrine regulator of adipocyte differentiation.[49] Thus, a major goal of the present study is to address whether this effect of CTRP11 on adipogenesis is physiologically relevant and, more broadly, whether this secreted protein is a *bona fide* regulator of whole body metabolism in vivo. A recent study also implicated a role for CTRP11/C1QL4 in steroidogenesis, based on the observations that recombinant CTRP11 can promote testosterone synthesis and secretion by TM3 Leydig cells and cultured seminiferous tubules.[50] Whether CTRP11 is required for testosterone production and secretion in the mouse testis was not determined. Additional role for CTRP11 in angiogenesis, based largely on in vitro studies, has also been noted[51]; the physiological relevance of these findings, however, remains uncertain.

Using biochemical and proteomics approaches, Bolliger et al. successfully identified Bai3/Adgrb3—a member of the adhesion GPCR family—as the cell surface receptor for CTRP11/C1QL4.[52] In the context of myogenesis, interaction of CTRP11 with BAI3 was shown to inhibit myoblast fusion.[38] Although BAI3 deficiency in mice negatively affects skeletal muscle fibers and muscle regeneration after injury,[38] it has not been determined whether the loss of CTRP11, the presumed ligand of BAI3 and a negative regulator of myogenesis, would similarly affect skeletal muscle fiber size and function.

Using a constitutive KO mouse model, we aimed to determine the physiological requirement of CTRP11 for maintaining metabolic homeostasis. Mice lacking CTRP11 appeared to have normal testosterone level and skeletal muscle weight and fiber size. Although grip strength was modestly reduced in CTRP11-null male, but not female, mice, locomotor function as assessed by rotarod tests was preserved. Loss of CTRP11, however, affected basal metabolic parameters, and glucose metabolism and insulin sensitivity in the obese state, in a sexually dimorphic manner. Furthermore, CTRP11 deficiency impaired metabolic flexibility as indicated by reduced fat loss when obese mice were subjected to obesity reversal by switching from a high-fat diet to a low-fat diet. Collectively, our results provided the first genetic evidence underscoring sexually dimorphic metabolic functions of CTRP11 in vivo.

2 | MATERIALS AND METHODS

2.1 | Mouse models

Mouse tissues from 8-week-old C57BL/6J male mice (The Jackson Laboratory, Bar Harbor, ME) were collected from fasted and refed experiments as previously described.[53] For the fasted group, food was removed for 16 h (beginning 10 h into the light cycle), and mice were euthanized 2 h into the light cycle. For the refed group, mice were fasted for 16 h and refed with chow pellets for 3 h before being euthanized. Tissues from C57BL/6J male mice fed a low-fat diet (LFD) or a high-fat diet (HFD) for 12 weeks were also collected as described.[53] The *Ctrp11*/*C1ql4* (B6;129S5-C1ql4^{tm1Lex}) knockout (KO) mouse strain was obtained from Taconic (Knockout Repository Model TF3851). To obtain a *Ctrp11*-null allele, a total of 552 bp covering the entire protein-coding region of exon 1 were replaced with a selection cassette. The original *Ctrp11*/*C1ql4*-null mice were generated on a mixed genetic background. We backcrossed and maintained the mice on a C57BL/6J genetic background for >6 generations. Genotyping primers for wild-type (WT) allele were forward (P36) 5′-CATTAGAACTGCACCCGAG GGTAA-3′ and reverse (P37) 5′-CACACCATGCGACAGCGACCTAGC-3′. The size of the WT band was 407 bp. Genotyping primers for the *Ctrp11* KO allele were forward (P36) 5′-CATTAGAACTGCACCCGAGGGTAA-3′ and reverse (GT-IRES) 5′-CCCTAGGAATGCTCGTCAAGA-3′. The size of the KO band was 553 bp. The genotyping PCR parameters were as follows: 94°C for 4 min, followed by 10 cycles of (94°C for 15 s, 65°C for 30 s, 72°C for 30 s), then

33 cycles of (94°C for 15 s, 55°C for 30 s, 72°C for 30 s), and lastly 72°C for 5 min. For the PCR genotyping reaction, 8% DMSO was included due to GC-rich sequences. Genotyping PCR products from WT and KO mice were excised and confirmed by DNA sequencing. All mice were generated by intercrossing *Ctrp11* heterozygous (+/-) mice. *Ctrp11* KO (-/-) and WT (+/+) littermate controls were housed in polycarbonate cages on a 12-h light–dark photocycle with ad libitum access to water and food. Mice were fed either a standard chow (Envigo; 2018SX), a high-fat diet (HFD; 60% kcal derived from fat; #D12492, Research Diets, New Brunswick, NJ), or a sucrose-matched control low-fat diet (LFD; 10% kcal derived from fat; #D12450J, Research Diets). Standard chow was provided for 12 weeks, beginning at 5 weeks of age. For the diet-induced obese group, HFD was provided for 20 weeks, beginning at 12 weeks of age. For the obesity reversal group, sucrose-matched LFD was provided for 4 weeks after the mice were on HFD for 20 weeks. At termination of the study, all mice were fasted for 2 h and euthanized. Tissues were collected, snap-frozen in liquid nitrogen, and kept at −80°C until analysis. All mouse protocols (protocol # MO19M48) were approved by the Institutional Animal Care and Use Committee of the Johns Hopkins University School of Medicine. All animal experiments were conducted in accordance with the National Institute of Health guidelines and followed the standards established by the Animal Welfare Acts.

2.2 | Body composition analysis

Body composition analyses for total fat, lean mass, and water content were determined using a quantitative magnetic resonance instrument (Echo-MRI-100, Echo Medical Systems, Waco, TX) at the Mouse Phenotyping Core facility at Johns Hopkins University School of Medicine.

2.3 | Complete blood count analysis

A complete blood count on blood samples was performed at the Pathology Phenotyping Core at Johns Hopkins University School of Medicine. Tail vein blood was collected using EDTA-coated blood collection tubes (Sarstedt, Nümbrecht, Germany) and analyzed using Procyte Dx analyzer (IDEXX Laboratories, Westbrook, ME).

2.4 | Indirect calorimetry

Chow or HFD-fed WT and *Ctrp11* KO male and female mice were used for simultaneous assessments of daily body weight change, food intake (corrected for spillage), physical activity, and whole body metabolic profile in an open flow indirect calorimeter (Comprehensive Laboratory Animal Monitoring System, CLAMS; Columbus Instruments, Columbus, OH) as previously described.[15] In brief, data were collected for 3 days to confirm mice were acclimatized to the calorimetry chambers (indicated by stable body weights, food intakes, and diurnal metabolic patterns), and data were analyzed from the fourth day. Rates of oxygen consumption ($\dot{V}_{O2}$; ml kg^{-1} h^{-1}) and carbon dioxide production ($\dot{V}_{CO2}$; ml kg^{-1} h^{-1}) in each chamber were measured every 24 min. Respiratory exchange ratio (RER = $\dot{V}_{CO2}/\dot{V}_{O2}$) was calculated by CLAMS software (version 4.02) to estimate relative oxidation of carbohydrates (RER = 1.0) versus fats (RER = 0.7), not accounting for protein oxidation. Energy expenditure (EE) was calculated as EE = $\dot{V}_{O2} \times [3.815 + (1.232 \times \text{RER})]$ and normalized to lean mass. Physical activities were measured by infrared beam breaks in the metabolic chamber. Average metabolic values were calculated per subject and averaged across subjects for statistical analysis by Student's *t*-test. Meal pattern data were analyzed for average meal frequency and meal size; a meal was defined as being at least 0.04 g and having a post-meal intermeal interval of at least 10 min, as previously described.[18,54] A food intake event was considered a meal only when both criteria were met. Intermeal interval was defined as time between consecutive meals. Satiety ratio was defined as intermeal interval divided by meal size (min/g).

2.5 | Glucose, insulin, and lipid tolerance tests

For glucose tolerance tests (GTTs), mice were fasted for 6 h before glucose injection. Glucose (Sigma, St. Louis, MO) was reconstituted in saline (0.9 g NaCl/L), sterile-filtered, and injected intraperitoneally (i.p.) at 1 mg/g body weight. Blood glucose was measured at 0, 15, 30, 60, and 120 min after glucose injection using a glucometer (NovaMax Plus, Billerica, MA). For insulin tolerance tests (ITTs), food was removed 2 h before insulin injection. Insulin was diluted in saline, sterile-filtered, and injected i.p. at 1.0 U/kg body weight, with the exception of a 1.2 U/kg body weight dosage used for male mice on HFD. Blood glucose was measured at 0, 15, 30, 60, and 90 min after insulin injection using a glucometer (NovaMax Plus). For lipid tolerance tests (LTTs), mice were fasted overnight (~16 h), then i.p. injected with 20% emulsified intralipid (soybean oil; MilliporeSigma) at a dose of 10 ul/g body weight. Blood was collected from the tail vein into capillary blood collection tubes before injection and 1, 2, 3, and 4 h post-injection. Serum was isolated from blood samples and assayed for TG using an Infinity kit (Thermo Fisher Scientific, Middletown, VA).

2.6 | Blood and tissue chemistry analysis

Tail vein blood samples were allowed to clot on ice and then centrifuged for 10 min at 10,000*g*. Serum samples were stored at −80°C until analyzed. Serum and liver triglycerides (TG) and cholesterol were measured according to manufacturer's instructions using an Infinity kit (Thermo Fisher Scientific, Middletown, VA). Non-esterified free fatty acids (NEFA) were measured using a Wako kit (Wako Chemicals, Richmond, VA). Serum β-hydroxybutyrate (ketone) concentrations were measured with a StanBio Liquicolor kit (StanBio Laboratory, Boerne, TX). Serum insulin (Crystal Chem, Elk Grove Village, IL; cat # 90080), testosterone (ALPCO, Salem, NH; cat# 55-TESMS-E01), IL-1β, IL-6, TNF-α, MCP-1/CCL2 (all from R&D Systems, Minneapolis, MN; cat # DY401-05, DY406-05, DY410-05, DY479-05) levels were measured by ELISA according to manufacturer's instructions.

2.7 | Hepatic lipid extraction

Mouse liver tissues (25 mg) were homogenized for 1 min in FastPrep tubes with 400 µl cold PBS using the FastPrep-24 bench-top bead beating lysis system (MP Biomedicals, Irvine, CA). 600 µl of cold PBS was added to each tube, then homogenized for another 1 min. 450 µl of the homogenate was aliquoted into a clear microtube. 500 µl of methanol and 500 µl of chloroform were added, and the resulting mixture was vortexed at 2500 rpm for 10–15 s. The mixture was spun at 3500 rpm for 5 min at room temperature. The bottom chloroform phase was transferred to a new clear tube by inverting the pipette tip through the middle protein layer without carrying the upper phase. The bottom chloroform phase was immediately dried under flowing nitrogen or air-dried overnight in the fume hood. The dried lipids were dissolved in appropriate volumes (either 4X or 10X of tissue weight) of chloroform. The resuspended lipids were stored at −80°C until used.

2.8 | Grip strength and rotarod tests

All behavioral tests were conducted during the dark cycle by experimenters blinded to genotypes. Motor coordination and learning was evaluated using the accelerating rotarod test as previously described.[55] Briefly, mice were placed on the rotarod (Columbus Instruments, Columbus, OH, USA) with a starting speed of 4 RPM, with an acceleration of 7.2 RPM/minute. The time at which each mouse dropped from the rotating rod was recorded. Each mouse was given three trials per day with a 2-min inter-trial interval, for 3 days. Grip strength was measured using a Bioseb grip strength meter (BIO-GS3, Bioseb, Pinellas Park, FL). Mice were held in front of a grid until the forepaws grabbed the grid. Mice were then pulled horizontally by the tail until they lost grip of the grid. Their peak pull force was recorded in each of three trials and averaged.

2.9 | Histology and quantification

Liver, gonadal (visceral) white adipose tissue, inguinal (subcutaneous) white adipose tissue, and gastrocnemius muscle were fixed in formalin. Paraffin embedding, tissue sectioning, and staining with hematoxylin and eosin were performed at the Pathology Core facility at Johns Hopkins University School of Medicine. Images were captured with a Keyence BZ-X700 All-in-One fluorescence microscope (Keyence Corp., Itasca, IL). Adipocyte and gastrocnemius cross-sectional area, as well as the total area covered by lipid droplets in hepatocytes, were measured on hematoxylin and eosin-stained slides using ImageJ software.[56] All cells in one field of view at 100X magnification per tissue section per mouse were analyzed. For muscle fiber cross-sectional area (CSA), at least 400 fibers were quantified per mouse. Image capturing and quantifications were carried out blinded to genotypes. Analyses were performed on a total of 17 male (WT, $n = 10$; KO, $n = 7$) HFD-fed mice.

2.10 | Quantitative real-time PCR analysis

Total RNA was isolated from tissues using Trizol reagent (Thermo Fisher Scientific) according to the manufacturer's instructions. Purified RNA was reverse transcribed using an iScript cDNA Synthesis Kit (Bio-rad). Real-time quantitative PCR analysis was performed on a CFX Connect Real-Time System (Bio-rad) using iTaq™ Universal SYBR Green Supermix (Bio-rad) per manufacturer's instructions. Data were normalized to either *β-actin* or *36B4* gene (encoding the acidic ribosomal phosphoprotein P0) and expressed as relative mRNA levels using the ΔΔCt method.[57] Fold change data were log-transformed to ensure normal distribution and statistics were performed. Real-time qPCR primers used to profile *Ctrp11* expression across different metabolic states were *Ctrp11* forward (m11-F), 5′-AAGGCCAAGATGAAGACAGCC-3′ and reverse (m11-R), 5′-GGTTTCATTGGATCCCAAGGT-3′; *36B4* forward, 5′-AGATTCGGGATATGCTGTTGGC-3′ and reverse, 5′-TCGGGTCCTAGACCAGTGTTC-3′. Additional qPCR primers used to further confirm the loss of *Ctrp11* transcript in KO mouse tissues were *Ctrp11* forward (m11-F2), 5′-ATTGCCTTCTACGCGGGTCTAA

GGCG-3′ and reverse (m11-R2), 5′-GCTGGTACCGTC ACCGCCTCGCA TG-3′. All other qPCR primers used were previously published.[13]

2.11 | Statistical analyses

All results are expressed as mean ± standard error of the mean (SEM). Statistical analysis was performed with Prism 9 software (GraphPad Software, San Diego, CA). Data were analyzed with two-tailed Student's *t*-tests or by repeated measures ANOVA. For two-way ANOVA, we performed Bonferroni post hoc tests. $p < .05$ was considered statistically significant.

3 | RESULTS

3.1 | Dynamic expression of *Ctrp11* across tissues in response to altered nutritional and metabolic state

To uncover whether CTRP11 has any potential metabolic role in vivo, we first assessed its expression across tissues in two opposing metabolic states, fasting and refeeding. In the refeeding phase, following overnight food deprivation, we observed a significant reduction in *Ctrp11* expression in gonadal (visceral) white adipose tissue, liver, skeletal muscle, kidney, and the hippocampus (Figure 1A). In contrast, when mice were chronically fed a high-fat diet to induce obesity, *Ctrp11* expression was significantly upregulated in the subcutaneous (inguinal) white adipose tissue, brown adipose tissue, heart, and small intestine relative to lean mice fed a matched control low-fat diet (Figure 1B). In liver, kidney, and skeletal muscle, chronic high-fat feeding downregulated *Ctrp11* expression (Figure 1B). These data indicate that *Ctrp11* expression is responsive to changes in nutritional and metabolic states.

3.2 | Generation of CTRP11-deficient mouse model

We used a constitutive knockout (KO) mouse model to determine whether CTRP11 is required for metabolic homeostasis in vivo. To ensure a complete null allele, exon 1 of the *Ctrp11* gene that encodes 75% of the entire protein (including the initiating methionine) was replaced with a selectable marker cassette (Figure 2A). PCR genotyping and sequencing confirmed the WT, heterozygous, and homozygous KO alleles (Figure 2B). Adipose tissue robustly expressed *Ctrp11* transcript.[49] As expected, based on the gene targeting strategy, *Ctrp11* transcript was not detected in the inguinal white adipose tissue of KO mice (Figure 2C). Previous studies have suggested a role for CTRP11/C1QL4 in testosterone synthesis[50] and skeletal myoblast fusion[38]; deficit in these two processes would likely confound our metabolic analysis and affect the metabolic outcomes of the *Ctrp11* KO mice. Measurements of serum testosterone levels in sexually mature male mice did not reveal any significant genotypic difference (Figure 2D). Grip strength was modestly reduced in male, but not female, KO mice relative to WT littermates (Figure 2E). Assessment of locomotor function using rotarod tests, however, did not reveal any significant difference between genotypes of either sex (Figure 2F). Although grip strength was modestly reduced in the *Ctrp11* KO male mice, skeletal muscle (gastrocnemius) histology and fiber size quantification did not reveal any genotypic difference

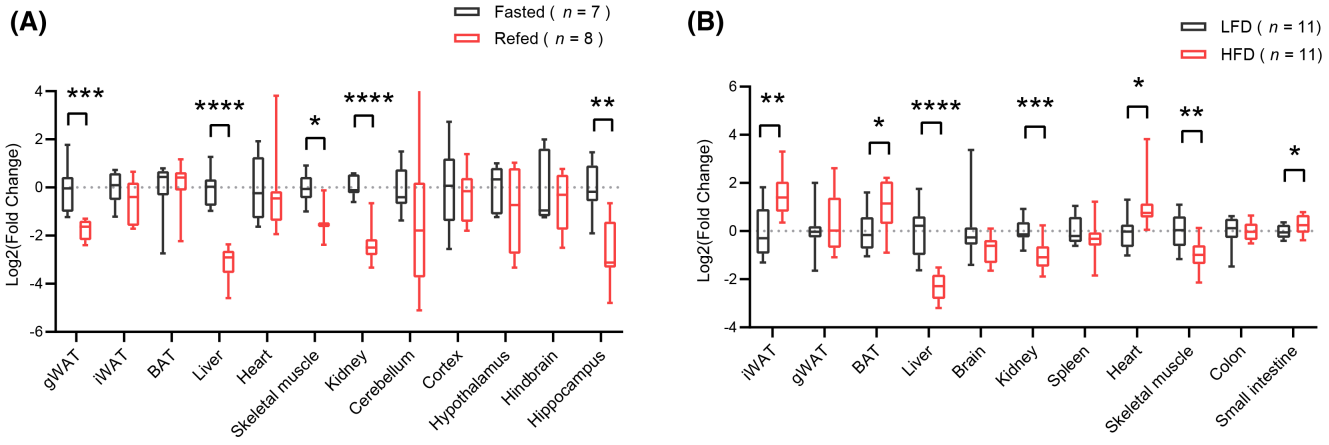

FIGURE 1 *Ctrp11* expression is regulated by nutritional and metabolic states. (A) Expression of *Ctrp11* in different mouse tissues in response to overnight (~16 h) food withdrawal and 3-h refeeding (after an overnight food deprivation). (B) Expression of *Ctrp11* in different mouse tissues in response to a 12-week period of control low-fat diet (LFD) or a high-fat diet (HFD). All data are presented as mean ± SEM. *$p < .05$; **$p < .01$; ***$p < .001$; ****$p < .0001$

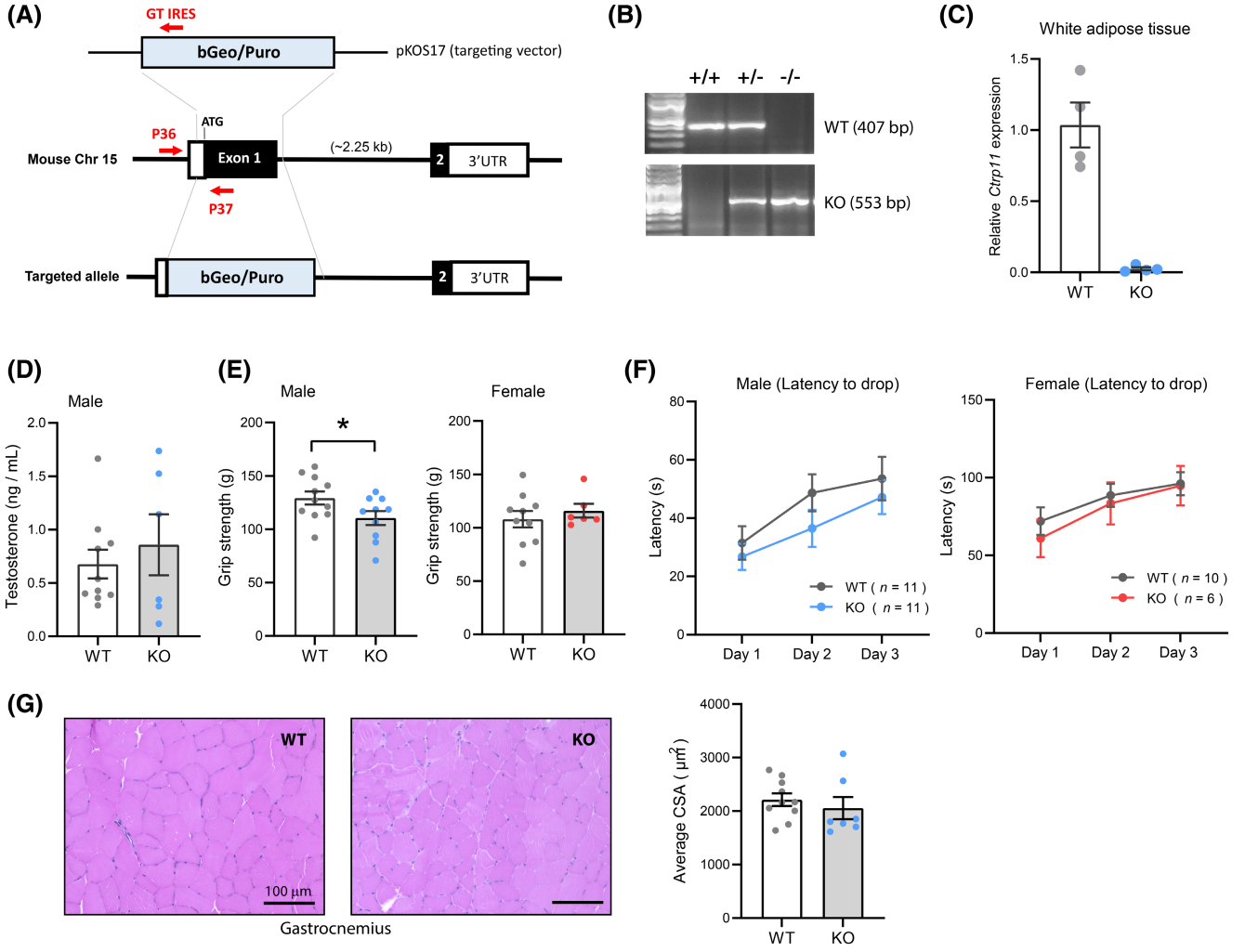

FIGURE 2 CTRP11-null mice have normal testosterone level and locomotor function. (A) Gene targeting strategy used to generate *Ctrp11* knockout (KO) mice. Exon 1 that encodes 179 amino acids (75% of the entire coding region) was replaced by the bGEO (a fusion of the β-galactosidase and neomycin resistance genes) and Puro (Puromycin resistance gene) cassette. The strategy ensures a complete null allele. The location of the forward (P36) and reverse (P37 and GT-IRES) primers used to genotype the wild-type (WT) and KO mice are indicated by the red arrows. (B) Representative PCR genotyping results indicating the successful generation of WT (+/+), heterozygous (+/–), and homozygous KO (–/–) mice. (C) Quantitative real-time PCR analysis confirming the complete absence of *Ctrp11* transcript in inguinal white adipose tissue of male mice. (D) Serum testosterone levels in WT ($n = 10$) and KO ($n = 7$) male mice at ~24 weeks of age. (E) Grip strength analysis of male (WT, $n = 11$; KO, $n = 10$) and female (WT, $n = 10$; KO, $n = 6$) mice. (F) Rotarod analysis of locomotor function in male and female WT and *Ctrp11* KO mice. (G) Representative gastrocnemius histology and the quantification of muscle fiber cross-sectional area (CSA) in WT ($n = 10$) and KO ($n = 7$) male mice at ~24 weeks of age. All data are presented as mean ± SEM. *$p < .05$

in male mice (Figure 2G). Measurements of gastrocnemius weight at the end of the study also revealed no significant difference between genotypes (Table S1). These data indicate that CTRP11 is dispensable for testosterone synthesis, skeletal muscle development, and locomotor function.

3.3 | CTRP11 deficiency elevates fasting serum ketone levels in female mice

Under the basal state when mice were fed a standard chow, CTRP11 deficiency did not affect body weight, body composition (fat and lean mass), fasting blood glucose and insulin levels, fasting serum lipid profiles, glucose tolerance and insulin sensitivity between WT and KO mice of either sex (Figure 3). One metabolic parameter that was significantly different between WT and KO mice is the marked elevation in serum ketones (β-hydroxybutyrate) in response to an overnight food withdrawal (Figure 3F). This effect was sex dependent and only observed in KO female, but not male, mice. Except for ketone, these data indicate that CTRP11 is largely dispensable for systemic glucose and lipid homeostasis under the basal state.

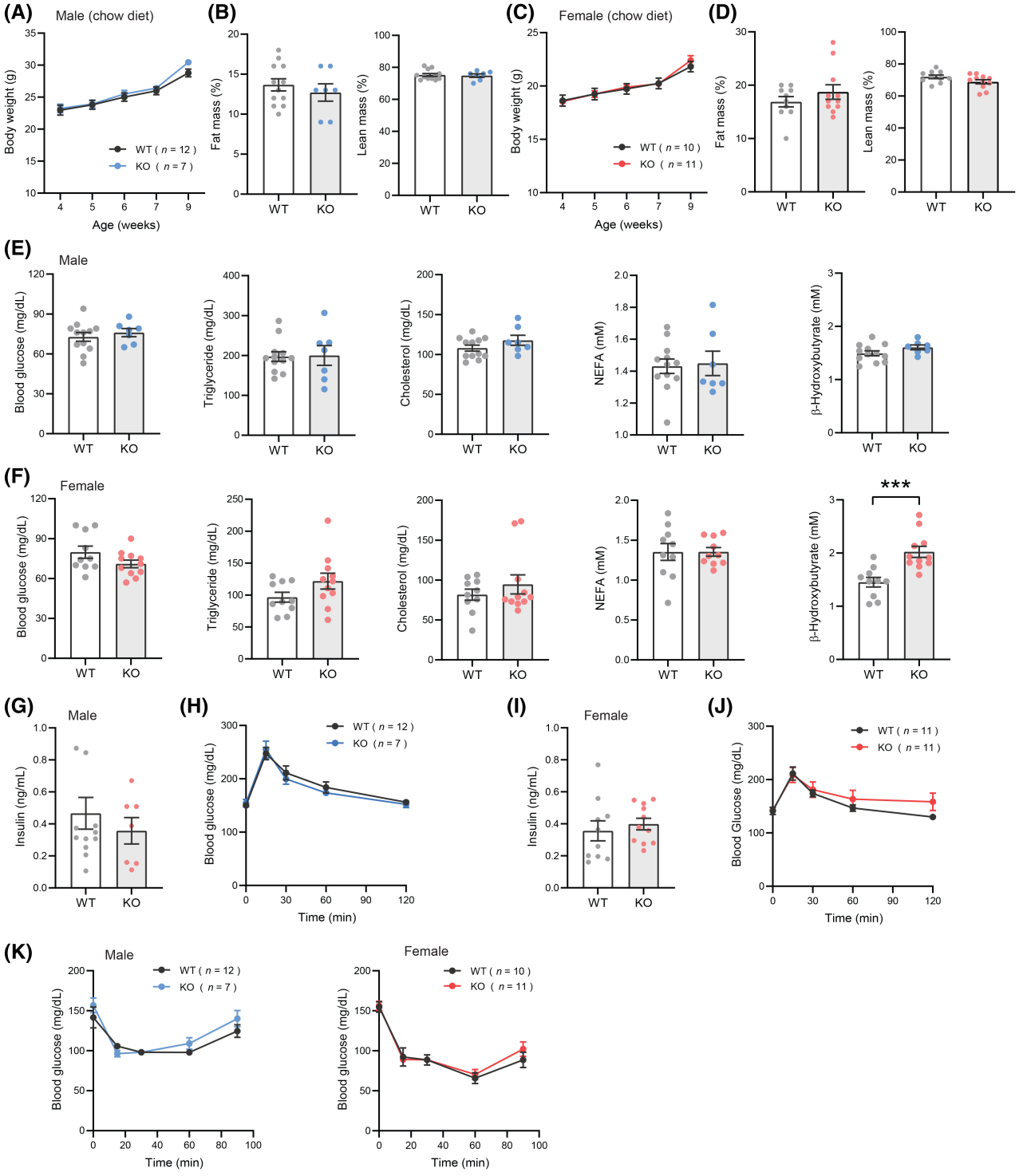

FIGURE 3 Basal metabolic profiles of WT and *Ctrp11*-KO mice fed a standard chow. (A) Body weights of WT littermates and *Ctrp11* KO male mice fed a standard chow over time (WT, $n = 12$; KO, $n = 7$). (B) Body composition analysis of % fat mass (relative to body weight) and % lean mass (relative to body weight) of WT and KO male mice. (C) Body weights of WT littermates and *Ctrp11* KO female mice fed a standard chow over time (WT, $n = 10$; KO, $n = 11$). (D) Body composition analysis of fat mass and lean mass of WT and KO female mice. (E) Overnight fasted serum glucose, triglyceride, cholesterol, non-esterified free fatty acids (NEFA), and β-hydroxybutyrate in WT and KO male mice. (F) Overnight fasted serum glucose, triglyceride, cholesterol, non-esterified free fatty acids (NEFA), and β-hydroxybutyrate in WT and KO female mice. (G) Fasted (6 h) serum insulin levels in WT and KO male mice. (H) Blood glucose levels during glucose tolerance tests in WT and KO male mice. (I) Fasted (6 h) serum insulin levels in WT and KO female mice. (J) Blood glucose levels during glucose tolerance tests in WT and KO female mice. (K) Blood glucose levels during insulin tolerance tests in male and female WT and KO mice. All data are presented as mean ± SEM. ***$p < .001$

3.4 | Loss of CTRP11 alters fasting–refeeding response in female mice

Indirect calorimetry was used to assess food intake, fuel utilization, and physical activity across the dark and light cycles in three different physiological states—ad libitum fed state, 24-h food deprivation, and refeeding period when food was reintroduced. Chow-fed male mice lacking CTRP11 were indistinguishable from WT littermates in food intake, oxygen consumption rate (VO_2), energy expenditure, and ambulatory activity across the different metabolic states and circadian cycles (Figure S1). In contrast, loss of CTRP11 significantly altered fasting–refeeding response in chow-fed KO female mice relative to WT littermates (Figure 4). Specifically, female mice lacking CTRP11 had reduced food intake, increased oxygen consumption rate (VO_2), and energy expenditure during the refeeding period when food was reintroduced after a 24-h food withdrawal (Figure 4C,F,I). In addition, CTRP11-deficient female mice also had markedly reduced ambulatory activity relative to WT littermates during the active (dark) cycle (Figure 4J,K). We conducted meal pattern analysis to determine which aspect of ingestive behavior is responsible for altered food intake across the fasting–refeeding cycle. Reduced food intake in the refeeding phase likely contributed by a smaller meal size and shorter meal duration (Figure 5), although these data fell short of reaching significance. Intermeal interval and satiety ratio were higher in female KO mice, whereas meal number and ingestion rate were not significantly different between genotypes (Figure 5). Together, these data indicate that CTRP11 is required for normal fasting–refeeding response and ambulatory activity in female mice.

3.5 | CTRP11 deficiency exacerbates obesity-induced glucose intolerance and insulin resistance

Next, we asked whether CTRP11 is required for metabolic homeostasis under the pathophysiological state of diet-induced obesity. When fed a high-fat diet (HFD), both male and female KO mice tended to gain slightly more weight over time relative to WT littermates (Figure 6A,C). Body composition analysis, however, did not reveal significant differences in fat and lean mass (normalized to body weight) between genotypes of either sex (Figure 6B,D). Glucose tolerance tests were performed to assess the capacity of the WT and KO mice to handle an acute glucose load. Loss of CTRP11 significantly exacerbated obesity-linked glucose intolerance in both male and female KO mice relative to WT littermates, with a more pronounced effect seen in the male mice (Figure 6E,F,H,I). Differences seen in glucose tolerance tests were not due to altered insulin levels; measurements of serum insulin before (time 0) and at 15 min post glucose injection revealed no significant difference between genotypes of either sex (Figure 6G,J). Insulin tolerance tests were conducted to directly assess systemic insulin sensitivity. Male mice lacking CTRP11 showed a more blunted response to insulin injection relative to WT controls, indicative of elevated obesity-induced insulin resistance (Figure 6K,L). Consistent with the modest decrease in glucose tolerance seen in the female KO mice (Figure 6H), insulin tolerance tests did not reveal any difference in insulin sensitivity between WT and KO female mice (Figure 6M,N). The exacerbated glucose intolerance and insulin resistance seen in the male KO mice, relative to WT controls, were not due to altered systemic inflammatory profile, as serum IL-1β, IL-6, TNF-α, and MCP-1/CCL2 levels were not significantly different between genotypes (Figure 6O).

3.6 | Loss of CTRP11 did not affect adipose and liver histology and gene expression

Reduced glucose tolerance and insulin sensitivity seen in male KO mice were not associated with adipocyte cell size in both visceral (gonadal) and subcutaneous (inguinal) fat depots (Figure 7A,B). It is known that chronic obesity results in marked infiltration of macrophages into fat depots,[58] as well as the development of adipose tissue fibrosis and oxidative stress.[59,60] Analyses of gene expression associated with pro-inflammatory M1 macrophage, anti-inflammatory M2 macrophage, fibrosis, and oxidative stress in visceral (gonadal) and subcutaneous (inguinal) white adipose tissue did not reveal any differences between genotypes (Figure 7C,D). Histological analysis and quantification also did not reveal any difference in the degree of hepatic steatosis (Figure 7E,F). Except for a modest reduction in hepatic expression of arginase 1 (Arg1), which is a marker of anti-inflammatory M2 macrophage, none of the other inflammatory, fibrotic, and oxidative genes in liver were significantly different between genotypes (Figure 7G). At the end of the high-fat study, organ weights were collected (Table S1). Except for a modest increase in % fat mass (inguinal fat depot normalized to body weight) seen in male KO mice, none of the organ weights (liver, heart, kidney, gonadal fat depot, gastrocnemius) were significantly different between genotypes of either sex (Table S1). These data indicate that CTRP11 deficiency worsens obesity-induced glucose intolerance and insulin resistance.

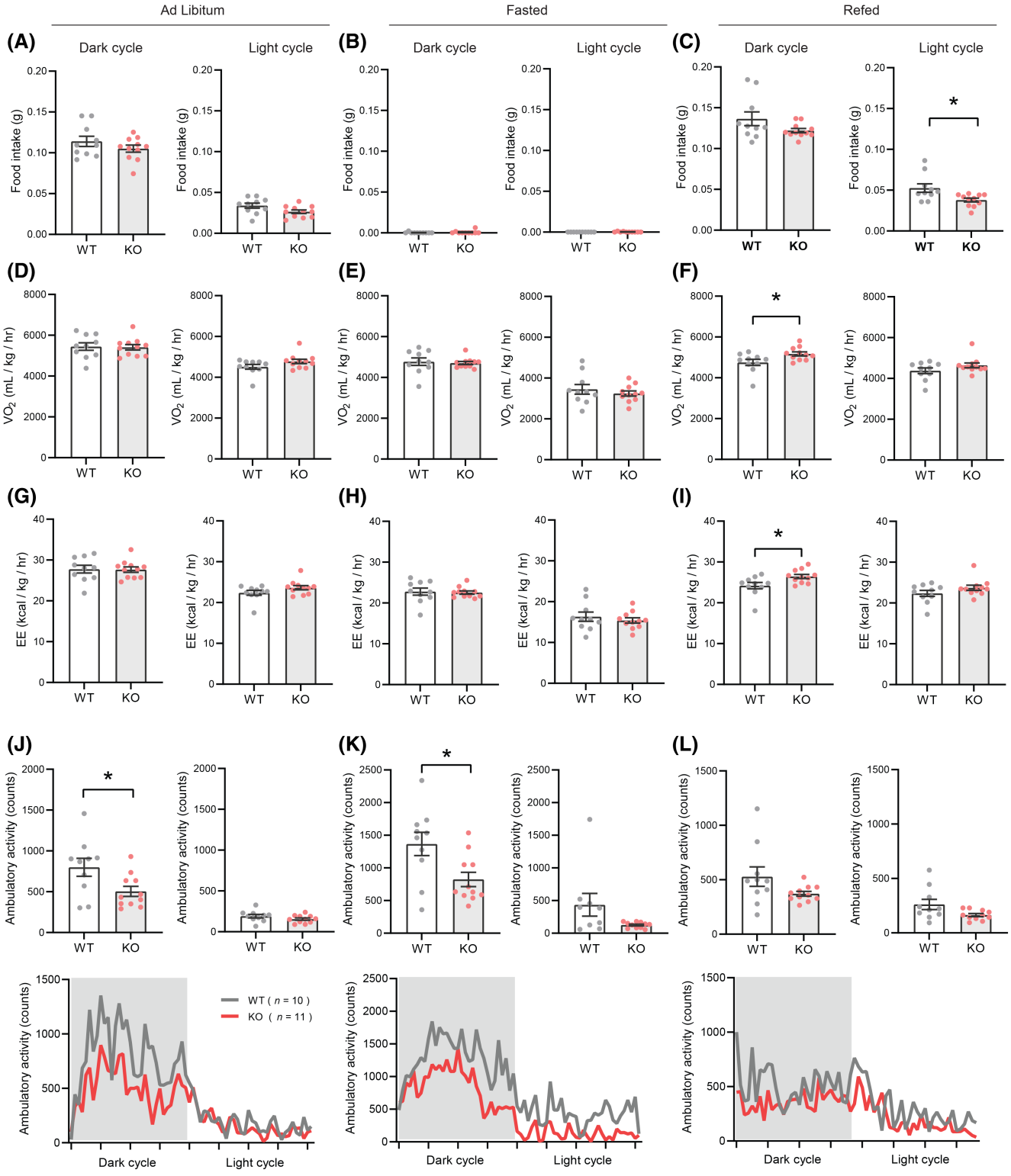

FIGURE 4 Food intake, oxygen consumption, energy expenditure, and physical activity of chow-fed WT and *Ctrp11*-KO female mice under ad libitum fed, fasted, and refed states. Indirect calorimetry analyses of WT littermates and KO female mice. Dark and light cycle food intake during ad libitum (A), food withdrawal (B), and refeeding phase (C). Dark and light cycle oxygen consumption rate (VO_2) during ad libitum (D), food withdrawal (E), and refeeding phase (F). Dark and light cycle energy expenditure (EE) during ad libitum (G), food withdrawal (H), and refeeding phase (I). Dark and light cycle ambulatory activity levels during ad libitum (J), food withdrawal (K), and refeeding phase (L). Oxygen consumption rate and energy expenditure data were normalized to lean mass. All data are presented as mean ± SEM. *$p < .05$. WT ($n = 10$); KO ($n = 11$)

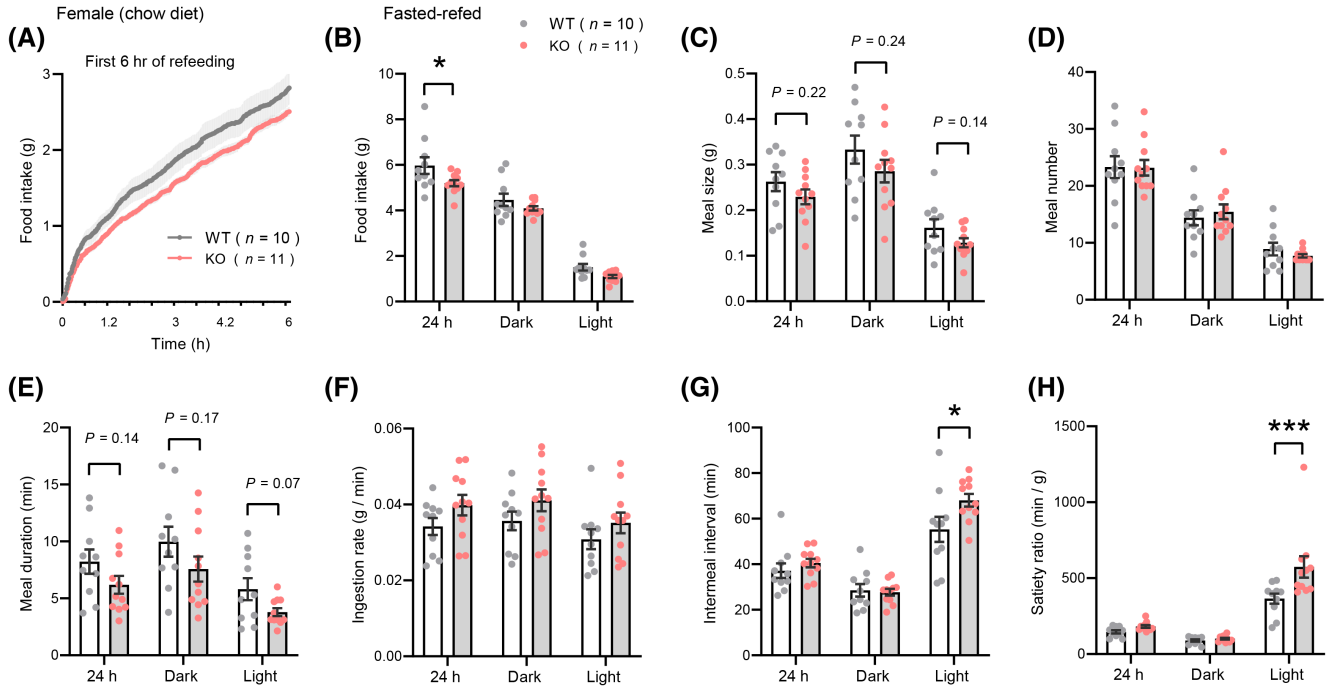

FIGURE 5 Meal pattern analysis of chow-fed *Ctrp11* KO female mice in the refed period following food deprivation. (A) Food intake in the first 6 h when food was reintroduced after a 24-h food withdrawal. (B) Total food intake in the light and dark cycle, as well as, over the 24-h period. (C) Meal size, (D) meal number, (E) meal duration, (F) ingestive rate, (G) intermeal interval, and (H) satiety ratio in WT ($n = 10$) and KO ($n = 11$) female mice. All data are presented as mean ± SEM. *$p < .05$; ***$p < .001$

3.7 | CTRP11-deficient male mice have reduced total white blood cell and lymphocyte count

Obesity is frequently associated with changes in blood cell composition due to local and systemic low-grade inflammation.[61,62] We thus assessed whether CTRP11 deficiency impacted blood cell composition. In HFD-fed male mice, loss of CTRP11 elevated reticulocyte counts and reduced total white blood cell (WBC) and lymphocyte counts (Table S2). In HFD-fed female KO mice, however, hemoglobin levels and hematocrit were elevated relative to WT controls (Table S2). These data indicate that CTRP11 deficiency alters blood cell composition in the context of diet-induced obesity.

3.8 | Loss of CTRP11 elevates cholesterol level but is dispensable for lipid homeostasis in the obese state

Given that *Ctrp11* expression is regulated by fasting and refeeding, and by chronic high-fat feeding (Figure 1), we assessed whether CTRP11 plays a role in regulating serum metabolite levels across the fasting–refeeding cycle in the diet-induced obese state. As expected, blood glucose and serum insulin and triglyceride levels rose in the refeeding period relative to the overnight fasted state, whereas ketones and non-esterified free fatty acid levels decreased (Figure 8A–L). The metabolite changes during this fasting–refeeding response were not significantly different between genotypes of either sex (Figure 8A–L). We noted, however, that fasting serum cholesterol levels were significantly higher in KO female, but not male, mice relative to WT controls (Figure 8J). We performed lipid tolerance tests to directly assess the capacity of the HFD-fed WT and KO mice to handle an acute lipid load. The kinetics of the rise and subsequent clearance of serum triglycerides following an intralipid infusion were indistinguishable between WT and KO mice of either sex (Figure 8M,N). These data indicate that CTRP11 deficiency results in a higher fasting cholesterol level, but is otherwise dispensable for lipid homeostasis in obese mice fed a high-fat diet.

3.9 | Altered fasting–refeeding response in lean *Ctrp11* KO female mice is lost in the obese state

Under the basal state when lean mice were fed a standard chow, loss of CTRP11 altered food intake, energy expenditure, and physical activity in response to fasting and refeeding (Figure 4). Using indirect calorimetry, we again

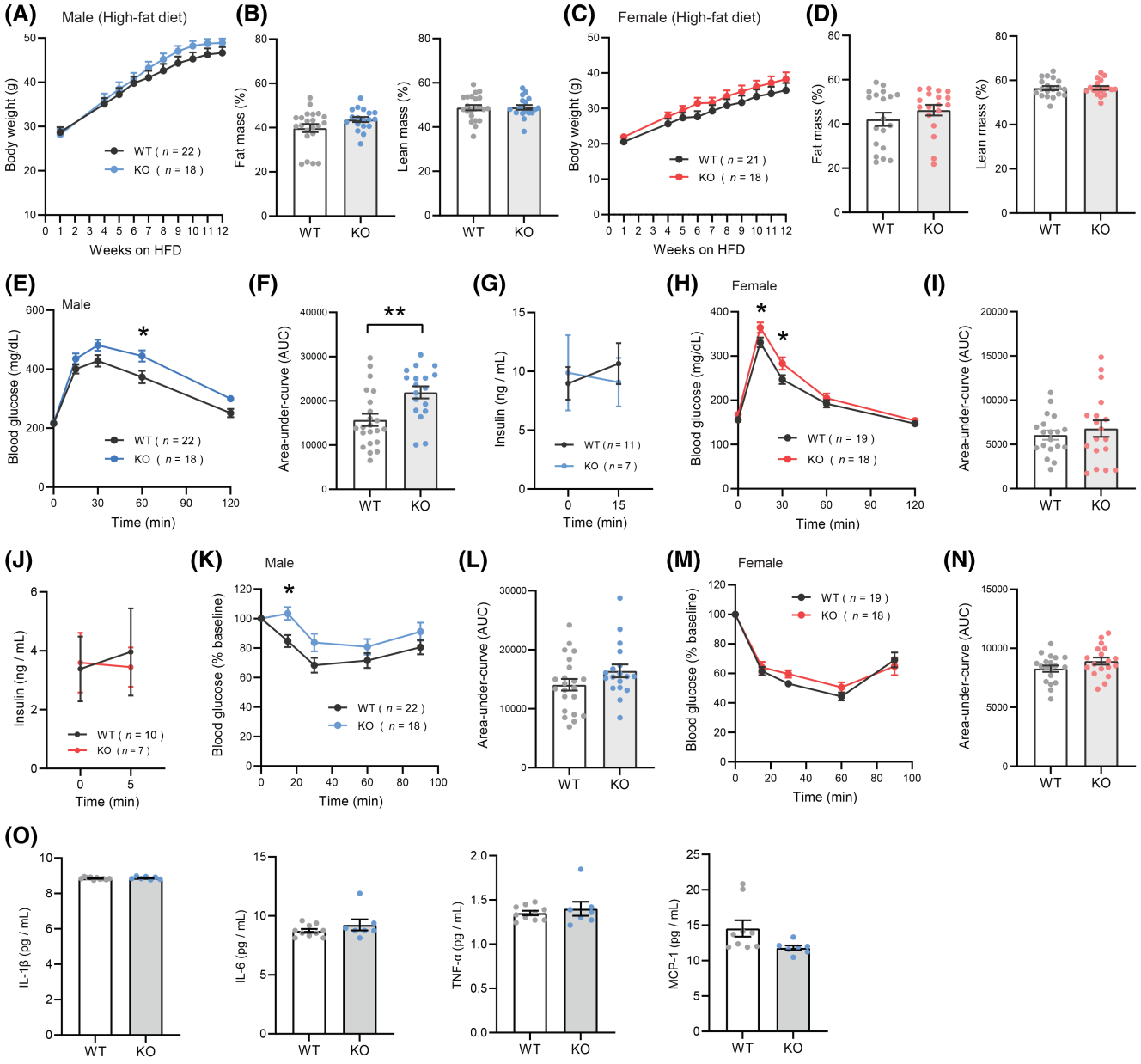

FIGURE 6 Metabolic profiles of WT and *Ctrp11*-KO mice fed a high-fat diet. (A) Body weights of WT littermates and *Ctrp11* KO male mice fed a high-fat diet (HFD) over time (WT, $n = 22$; KO, $n = 18$). (B) Body composition analysis of % fat mass (relative to body weight) and % lean mass (relative to body weight) of WT and KO male mice. (C) Body weights of WT littermates and *Ctrp11* KO female mice fed HFD over time (WT, $n = 21$; KO, $n = 18$). (D) Body composition analysis of % fat mass and % lean mass of WT and KO female mice. (E) Blood glucose levels during glucose tolerance tests in WT and KO male mice. (F) Area under curve for data shown in E. (G) Serum insulin levels at time 0 and 15 post glucose injection in male mice. (H) Blood glucose levels during glucose tolerance tests in WT and KO female mice. (I) Area under curve for data shown in H. (J) Serum insulin levels at time 0 and 15 post glucose injection in female mice. (K) Blood glucose levels during insulin tolerance tests in WT and KO male mice. (L) Area under curve for data shown in K. (M) Blood glucose levels during insulin tolerance tests in WT and KO female mice. (N) Area under curve for data shown in M. (O) Serum inflammatory cytokine (IL-1β, IL-6, TNF-α, and MCP-1/CCL2) levels in WT ($n = 10$) and KO ($n = 7$) male mice. All data are presented as mean ± SEM. *$p < .05$

determined whether similar changes in whole body response to fasting–refeeding persisted in diet-induced obese KO female mice. Across the circadian cycles and in three different metabolic states (ad libitum fed, fasted, refed), we observed no significant differences in food intake, oxygen consumption rate, respiratory exchange ratio, energy expenditure, and physical activity between genotypes of either sex (Table S3). Thus, altered whole body fasting–refeeding response seen in chow-fed *Ctrp11* KO female mice was lost in the context of obesity induced by chronic high-fat feeding.

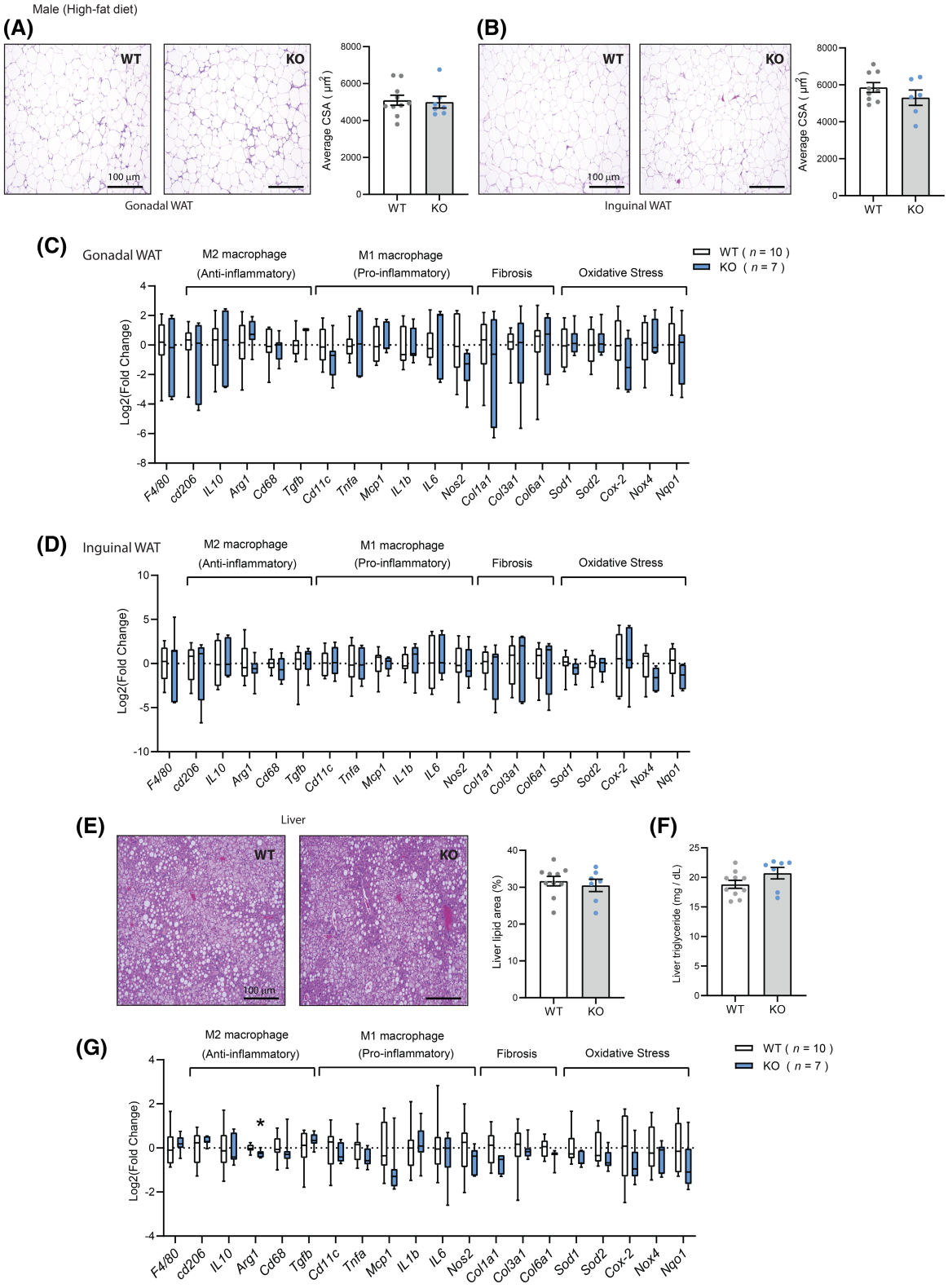

FIGURE 7 Tissue histology and gene expression in WT and *Ctrp11*-KO male mice fed a high-fat diet. (A) Representative histology of visceral (gonadal) white adipose tissues and the quantification of adipocyte cell size (cross-sectional area, CSA) in WT and KO male mice. (B) Representative histology of subcutaneous (inguinal) white adipose tissues and the quantification of adipocyte cell size (cross-sectional area, CSA) in WT and KO male mice. (C and D) Expression of anti-inflammatory M2 macrophage markers, pro-inflammatory M1 macrophage markers, fibrotic and oxidative stress genes in the gonadal white adipose tissue (C) and inguinal white adipose tissue (D) of WT and KO male mice. (E) Representative histology of liver tissues and the quantification of lipid area (% of total area) in WT and KO male mice. (F) Hepatic TG levels in WT and KO male mice. (G) Expression of anti-inflammatory M2 macrophage markers, pro-inflammatory M1 macrophage markers, fibrotic and oxidative stress genes in the liver of WT and KO male mice. All data are presented as mean ± SEM. *$p < .05$

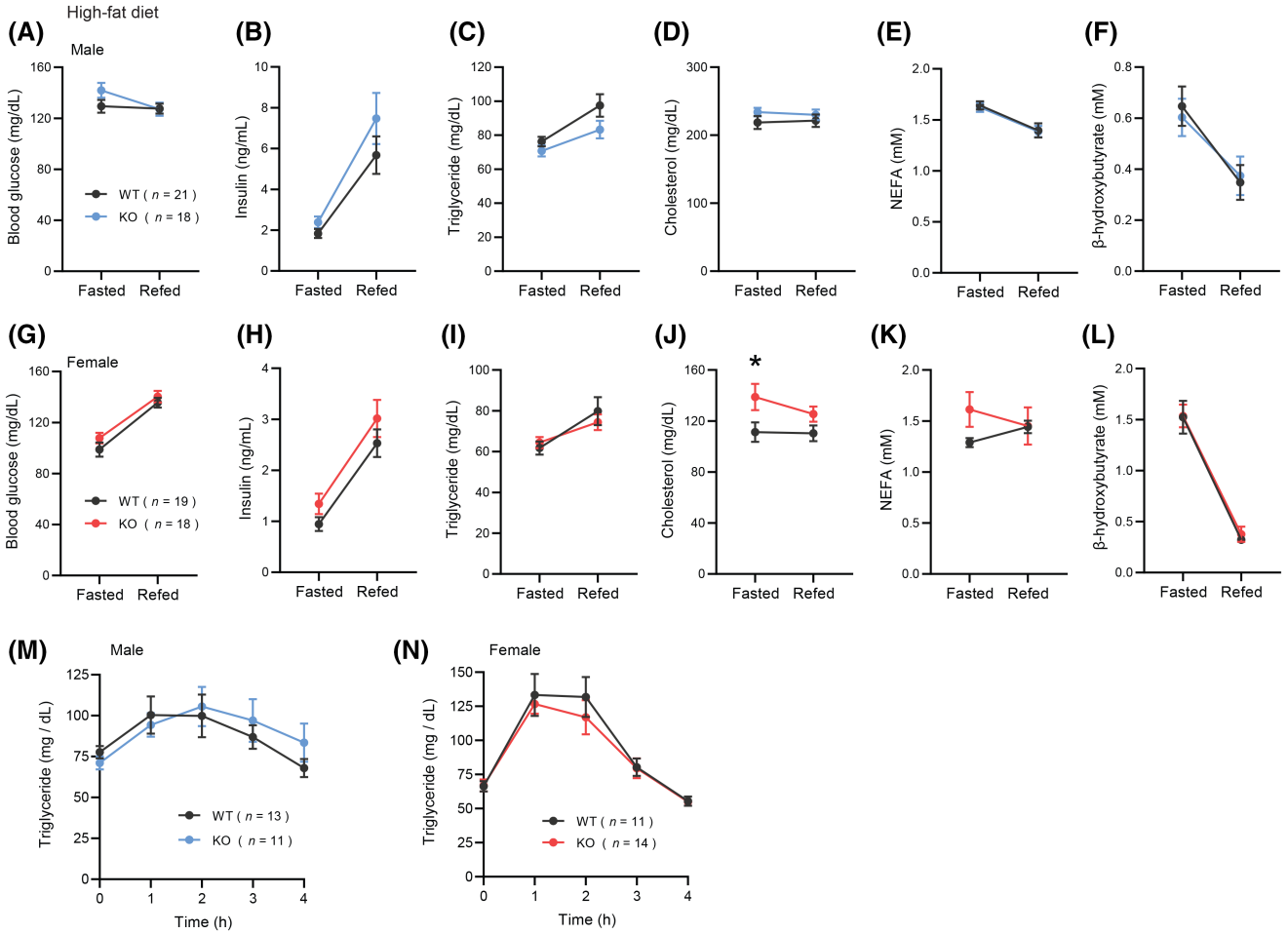

FIGURE 8 Fasting–refeeding lipid profiles and lipid tolerance tests of WT and *Ctrp11*-KO mice fed a high-fat diet. Blood glucose (A), serum insulin (B), triglyceride (C), cholesterol (D), non-esterified free fatty acids (NEFA; E), and β-hydroxybutyrate (F) levels in overnight fasted and 2 h refed WT ($n = 21$) and KO ($n = 18$) male mice on HFD. Blood glucose (G), serum insulin (H), triglyceride (I), cholesterol (J), non-esterified free fatty acids (NEFA; K), and β-hydroxybutyrate (L) levels in overnight fasted and 2 h refed WT ($n = 19$) and KO ($n = 18$) female mice on HFD. (M and N) Serum triglyceride levels during lipid tolerance tests in male (M) and female (N) WT and KO mice on HFD. All data are presented as mean ± SEM

3.10 | CTRP11 deficiency impairs fat loss in male mice subject to obesity reversal

We next examined metabolic flexibility of the *Ctrp11* KO mice by assessing how obese mice fed a HFD responded to diet reversal in which HFD was switched back to LFD for 4 weeks. Diet reversal did not significantly alter the expected body weight reduction between WT and KO male mice (Figure 9A). WT male mice, however, had a significantly greater loss of fat mass (normalized to body weight) compared to *Ctrp11* KO mice (Figure 9B). Lean mass was maintained in male mice subjected to obesity reversal (Figure 9C). No genotypic differences in body weight and body composition, however, were observed in female mice subject to obesity reversal (Figure 9D–F). The capacity to dispose of an acute glucose load as assessed by glucose tolerance tests was not different between WT and KO mice of either sex subject to obesity reversal (Figure 9G,H). Insulin tolerance tests indicated a moderate reduction in whole body insulin sensitivity in *Ctrp11* KO male mice relative to WT controls subject to obesity reversal (Figure 9I,J). No difference in insulin sensitivity was observed in female mice subject to obesity reversal (Figure 9K). Fasting blood glucose, serum insulin, triglyceride, cholesterol, non-esterified free fatty acid, and β-hydroxybutyrate levels were also not significantly different between genotypes of either sex subject to obesity reversal (Figure 9L,M). Obesity reversal also did not improve systemic inflammatory profiles (serum IL-1β, IL-6, TNF-α, and MCP-1) between WT and KO male mice

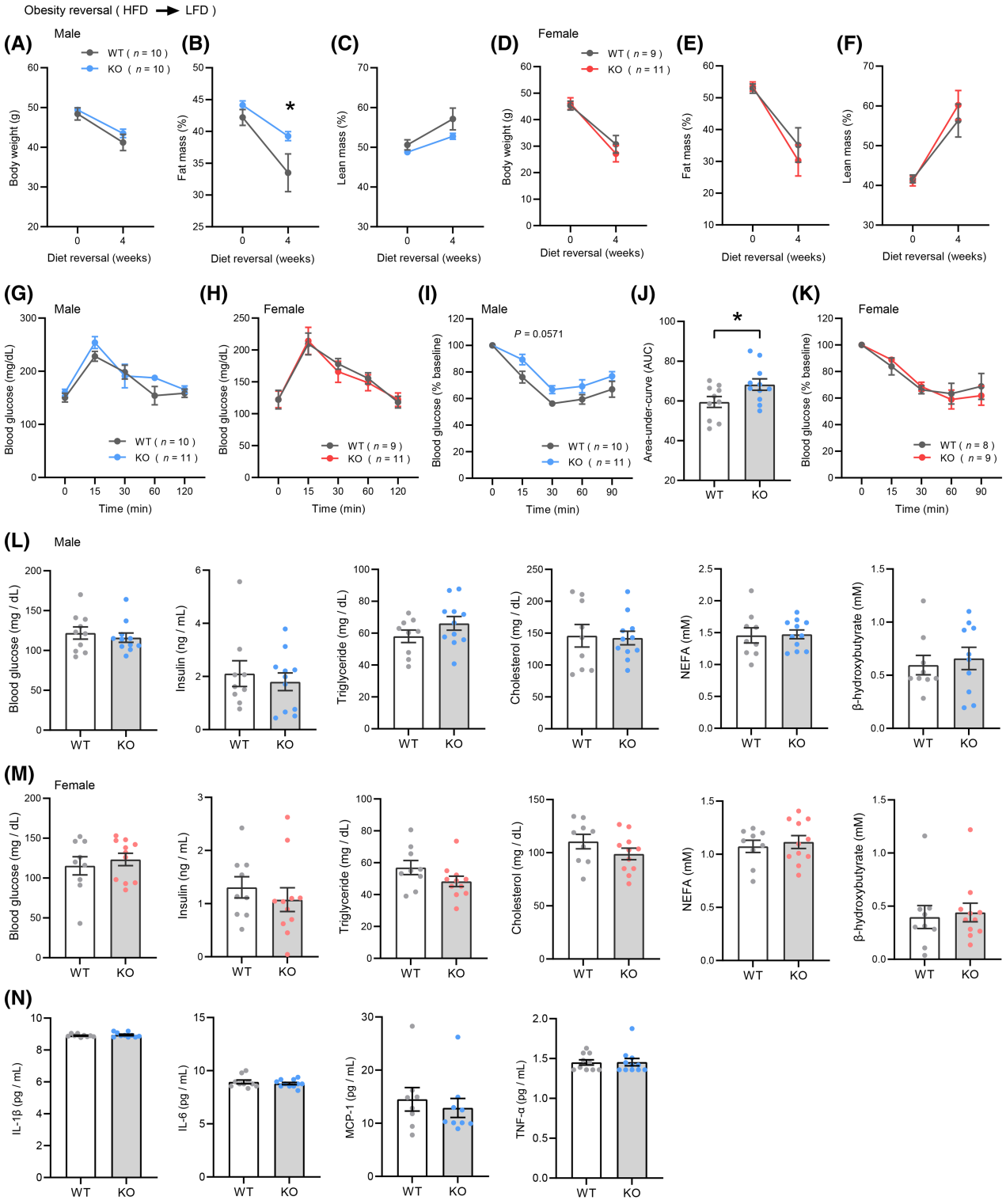

FIGURE 9 Metabolic profiles of obese WT and *Ctrp11*-KO mice subjected to obesity reversal. (A–F) Body weight and body composition (% fat mass and lean mass normalized to body weight) of HFD-induced obese male and female mice before (time 0) and after 4 weeks of diet reversal (switching from HFD to LFD). (G and H) Blood glucose levels during glucose tolerance tests in WT and KO male (G) and female (H) mice subjected to obesity reversal. (I) Blood glucose levels during insulin tolerance tests in male WT and KO mice subjected to obesity reversal. (J) Area under curve for data shown in I. (K) Insulin tolerance tests in female WT and KO mice subjected to obesity reversal. (L-M) Fasting (~16 h) blood glucose, serum insulin, triglyceride, cholesterol, non-esterified free fatty acids (NEFA), and β-hydroxybutyrate levels in male (L) and female (M) mice subjected to obesity reversal. (N) Serum IL-1β, IL-6, TNF-α, and MCP-1/CCL2 levels in WT and KO male mice. All data are presented as mean ± SEM. *$p < .05$. Male (WT, $n = 10$; KO, $n = 11$); Female (WT, $n = 9$; KO, $n = 11$)

(Figure 9N). These data indicate that CTRP11 is required for optimal fat loss in obese male mice subject to diet reversal, and its deficiency impairs normal responses to dietary intervention in obesity, but is otherwise dispensable for systemic glucose, lipid, and inflammatory profiles.

4 | DISCUSSION

In this study, we characterized the in vivo function of CTRP11 using a novel genetic loss-of-function mouse model, focusing on the contributions of CTRP11 to systemic metabolism. Our previous in vitro studies have suggested a potential role for CTRP11 as a negative paracrine regulator of adipogenesis.[49] We hypothesized that CTRP11 deficiency would likely impact fat mass in mice. Although the *Ctrp11* KO mice fed a HFD tended to be slightly heavier than WT littermates, loss of CTRP11 did not significantly alter whole body adiposity, even when adipocyte hypertrophy and hyperplasia were maximally induced by chronic high-fat feeding. Assuming the lack of compensatory response, our results indicate that CTRP11 is dispensable for modulating adipogenesis in vivo. The negative data on adiposity may not be entirely unexpected; there were instances notwithstanding the striking results on adipogenesis in vitro[63,64] in which genetic loss-of-function mouse models did not reveal the expected deficit or alteration in adiposity in vivo.[65,66] Given the inherent complexity of in vivo milieu, our observations reinforce and underscore the value of using genetic mouse models in confirming and validating in vitro findings in a physiologic context.

We noted the expression of *Ctrp11* is modulated by nutritional and metabolic states, suggestive of a metabolic role. Indeed, the *Ctrp11* KO mouse model has provided novel and valuable insights concerning its metabolic function. In chow-fed lean mice under the basal state, CTRP11 deficiency affected whole body metabolic parameters in a sexually dimorphic manner. Overnight food deprivation resulted in significantly higher serum ketones in *Ctrp11* KO female, but not male, mice. Since fasting-induced ketogenesis is linked to hepatic fat oxidation, our result suggests that CTRP11 may have a sex-dependent role in modulating hepatic fat oxidation and ketones production in the fasted state. Unlike male mice, *Ctrp11* KO female mice also had reduced food intake and increased oxygen consumption and energy expenditure in the refeeding period following a 24-h food withdrawal. Ambulatory activity in the ad libitum fed and fasted states was also significantly reduced in the active (dark) cycle of *Ctrp11* KO female mice, but not males. Interestingly, when *Ctrp11* KO female mice were chronically fed an HFD, the observed fasting–refeeding induced changes in food intake, oxygen consumption, energy expenditure, and physical activity initially noted in lean chow-fed mice were lost.

In the lean basal state, all the phenotypes observed were restricted to *Ctrp11* KO female mice, whereas CTRP11 was largely dispensable for metabolic control in chow-fed male mice. Conversely, in the HFD-induced obese state, most of the phenotypic differences between genotypes were seen in male, but not female, mice. In the context of diet-induced obesity, CTRP11 deficiency further exacerbated glucose intolerance and insulin resistance, effects that were significantly more pronounced in *Ctrp11* KO male compared to female mice. The mechanism that contributes to the further deterioration of systemic insulin sensitivity induced by HFD in *Ctrp11* KO male mice is unclear, as this phenotype was not associated with adiposity, adipocyte cell size, the extent of steatosis in the liver, or changes in gene expression related to inflammation, fibrosis, and oxidative stress. Total white blood cell and lymphocyte counts were modestly reduced in *Ctrp11* KO male mice. Since further analysis was not conducted, we therefore do not know which populations of pro- and anti-inflammatory immune cells in circulation are affected by CTRP11 deficiency. However, the serum levels of major inflammatory cytokines (IL-1β, IL-6, TNF-α, and MCP-1/CCL2), as well as their mRNA expression in fat depots and liver, were not different between genotypes, thus arguing against inflammation as a significant contributor of insulin resistance seen in the KO male mice.

Lastly, we subjected a group of diet-induced obese mice to obesity reversal to determine if CTRP11 plays a role in modulating metabolic response to dietary intervention. Obese female KO mice responded similar to WT littermates when subjected to diet reversal. In contrast, reversal to a low-fat diet after obesity induction resulted in significantly greater fat loss (relative to body mass) in WT littermates than in *Ctrp11* KO male mice. Accordingly, *Ctrp11* KO male mice with greater adiposity (after diet reversal) continued to be more insulin resistant compared to the WT littermates. These results indicate that loss of CTRP11 blunts the response of obese male mice to dietary intervention induced fat loss, suggesting that CTRP11 may directly or indirectly modulating metabolic flexibility, a phenomenon associated with reduced ability to respond to changes in metabolic demand and fuel selection.[67] Because indirect calorimetry was not conducted on the obesity reversal mice, we do not know whether switching from HFD to LFD differentially affects food intake patterns, metabolic rate, physical activity, and energy expenditure in WT and *Ctrp11* KO male mice.

One of the common themes that emerges from our studies of various CTRP KO mouse models is the importance of sex as a significant biological variable

that contributes to metabolic and phenotypic outcomes.[10,11,13–15,17,18,53,55,68] Depending on whether the mice are lean (chow-fed) or obese (HFD-fed), most of the metabolic alterations due to CTRP deficiency are often restricted to either male or female mice. Without the inclusion of both sexes in our phenotypic analyses of CTRP-deficient animals, we would have missed some of the important data highlighting the contributions of each CTRP family member to physiology and pathophysiology. While the loss of CTRP11 results in context-dependent and sexually dimorphic phenotypes, we do not know the mechanism of how sex hormones might be contributing to the observed sex-dependent phenotypes. Given the pleiotropic roles of sex hormones in regulating development and the postnatal function of central and peripheral organs, additional studies are needed to determine how sex hormone actions may influence fasting–refeeding response and insulin sensitivity in the context of CTRP11 deficiency. Nevertheless, the present study serves to reinforce the impact of sex on physiologic response to genetic manipulation in preclinical animal models and its relevance to clinical/translational research, an issue that has been raised repeatedly.[69–71]

Although not the focus of the study, we also assessed whether loss of CTRP11 affects testosterone synthesis and skeletal muscle development based on prior findings indicating a role for CTRP11 in these two processes.[38,50] Testosterone is a potent sex steroid with demonstrable effects on systemic metabolism.[72] Skeletal muscle, being the largest and metabolically active organ by mass, plays an especially important role in modulating systemic energy balance.[73] Thus, if sex steroid synthesis and/or muscle development and function were affected in the *Ctrp11* KO mice, it could affect our metabolic analysis. Testis and adipose tissue have the highest expression of *Ctrp11* relative to other tissues examined.[49] Contrary to expectation based on the in vitro results,[50] sexually mature *Ctrp11* KO male mice appeared to have normal serum testosterone levels, indicating that CTRP11 is not required for testosterone synthesis in vivo. This is perhaps not surprising. Many conserved genes that are highly and uniquely expressed in testis are postulated to have a role in various aspects of the male reproductive system; however, systematic deletion of these genes using CRISPR-Cas9 method revealed that almost all, when individually mutated, are not essential or required for reproductive competence.[74–76]

The binding of C1QL4 (CTRP11) to the adhesion GPCR (Bai3/Adgrb3) on muscle progenitor cells has been shown to inhibit myoblast fusion.[38] Mice lacking Bai3 have smaller myofibers and are less efficient at regeneration after cardiotoxin injury.[38] Because *Ctrp11* KO mice were not available in the previous study, we did not know whether the reciprocal also holds true, namely that the skeletal muscle of *Ctrp11* KO mice would phenocopy the Bai KO phenotype. Contrary to our expectation, mice lacking CTRP11 appeared to have normal skeletal muscle development, muscle mass (gastrocnemius), and myofiber size, indicating that CTRP11 is not essential for myogenesis. Consistent with this, rotarod test of locomotor function revealed no significant differences between WT and *Ctrp11* KO mice of either sex. However, we did observe a modest reduction in grip strength in *Ctrp11* KO male, but not female, mice. Additional studies are warranted to assess whether the modest reduction in grip strength seen in male KO mice will worsen with age. It would also be worthwhile in future studies to functionally stress the muscle of the *Ctrp11* KO mice in treadmill to determine whether loss of CTRP11 would affect the time it takes for the exercising muscle to get fatigued. We also do not know if skeletal muscle of *Ctrp11* KO mice would regenerate normally as the WT littermates if subjected to cardiotoxin injury. It should be noted that there is redundancy in the ligands that can engage Bai3.[52] In addition to C1QL4 (CTRP11), three other related family members (C1QL1/CTRP14, C1QL2/CTRP10, and C1QL3/CTRP13) have all been shown to bind with high affinity to Bai3.[52] Thus, it is possible that other related Bai3 ligands can functionally substitute for the complete absence of CTRP11.

A limitation and caveat of our study is the use of a constitutive KO mouse model. We do not know whether CTRP11 inactivation would induce compensatory response that could mask some of the metabolic phenotypes. For example, conditional inactivation of the widely studied insulin-sensitizing adipokine, adiponectin, in adult mice results in a much more dramatic metabolic outcomes compared to the constitutive adiponectin KO mouse models.[77] Thus, future studies employing a conditional KO model of CTRP11 in adult mice will help address the issue of compensation during development and early postnatal period, as well as the relative contribution of central and peripheral derived CTRP11 in modulating food intake, energy expenditure, and insulin sensitivity. In summary, despite the noted caveat and limitations, we provided the first physiological analysis and genetic evidence for novel sex-dependent metabolic regulations by CTRP11, particularly as it relates to fasting–refeeding response, glucose tolerance, and obesity reversal through dietary intervention.

ACKNOWLEDGMENTS

This work was supported by the National Institutes of Health (DK084171 to G.W.W.).

DISCLOSURES

The authors declare no conflicts of interest.

AUTHOR CONTRIBUTIONS

Dylan C. Sarver and GWW contributed to the experimental design; Dylan C. Sarver, Cheng Xu, Chantelle E. Terrillion, Susan Aja, and G. William Wong performed the experiments; Dylan C. Sarver, Chantelle E. Terrillion, Susan Aja, and G. William Wong analyzed and interpreted the data; G. William Wong drafted the paper with inputs and edits from all authors.

DATA AVAILABILITY STATEMENT

The data that support the findings of this study are included in the results section of this article. No additional datasets were generated or analyzed beyond what is described in this article.

REFERENCES

1. Reid KB, Porter RR. Subunit composition and structure of subcomponent C1q of the first component of human complement. *Biochem J*. 1976;155:19-23.
2. Ghai R, Waters P, Roumenina LT, et al. C1q and its growing family. *Immunobiology*. 2007;212:253-266.
3. Ressl S, Vu BK, Vivona S, Martinelli DC, Sudhof TC, Brunger AT. Structures of C1q-like proteins reveal unique features among the C1q/TNF superfamily. *Structure*. 2015;23:688-699.
4. Kishore U, Gaboriaud C, Waters P, et al. C1q and tumor necrosis factor superfamily: modularity and versatility. *Trends Immunol*. 2004;25:551-561.
5. Tom Tang Y, Hu T, Arterburn M, et al. The complete complement of C1q-domain-containing proteins in Homo sapiens. *Genomics*. 2005;86:100-111.
6. Seldin MM, Tan SY, Wong GW. Metabolic function of the CTRP family of hormones. *Rev Endocr Metab Disord*. 2014;15:111-123.
7. Wong GW, Krawczyk SA, Kitidis-Mitrokostas C, Revett T, Gimeno R, Lodish HF. Molecular, biochemical and functional characterizations of C1q/TNF family members: adipose-tissue-selective expression patterns, regulation by PPAR-gamma agonist, cysteine-mediated oligomerizations, combinatorial associations and metabolic functions. *Biochem J*. 2008;416:161-177.
8. Wong GW, Wang J, Hug C, Tsao TS, Lodish HF. A family of Acrp30/adiponectin structural and functional paralogs. *Proc Natl Acad Sci U S A*. 2004;101:10302-10307.
9. Lei X, Rodriguez S, Petersen PS, et al. Loss of CTRP5 improves insulin action and hepatic steatosis. *Am J Physiol Endocrinol Metab*. 2016;310:E1036-E1052.
10. Lei X, Seldin MM, Little HC, Choy N, Klonisch T, Wong GW. C1q/TNF-related protein 6 (CTRP6) links obesity to adipose tissue inflammation and insulin resistance. *J Biol Chem*. 2017;292:14836-14850.
11. Lei X, Wong GW. C1q/TNF-related protein 2 (CTRP2) deletion promotes adipose tissue lipolysis and hepatic triglyceride secretion. *J Biol Chem*. 2019;294:15638-15649.
12. Little HC, Rodriguez S, Lei X, et al. Myonectin deletion promotes adipose fat storage and reduces liver steatosis. *FASEB J*. 2019;33:8666-8687.
13. Petersen PS, Lei X, Wolf RM, et al. CTRP7 deletion attenuates obesity-linked glucose intolerance, adipose tissue inflammation, and hepatic stress. *Am J Physiol Endocrinol Metab*. 2017;312:E309-E325.
14. Rodriguez S, Lei X, Petersen PS, Tan SY, Little HC, Wong GW. Loss of CTRP1 disrupts glucose and lipid homeostasis. *Am J Physiol Endocrinol Metab*. 2016;311:E678-E697.
15. Sarver DC, Stewart AN, Rodriguez S, Little HC, Aja S, Wong GW. Loss of CTRP4 alters adiposity and food intake behaviors in obese mice. *Am J Physiol Endocrinol Metab*. 2020;319:E1084-E1100.
16. Seldin MM, Peterson JM, Byerly MS, Wei Z, Wong GW. Myonectin (CTRP15), a novel myokine that links skeletal muscle to systemic lipid homeostasis. *J Biol Chem*. 2012;287:11968-11980.
17. Tan SY, Lei X, Little HC, et al. CTRP12 ablation differentially affects energy expenditure, body weight, and insulin sensitivity in male and female mice. *Am J Physiol Endocrinol Metab*. 2020;319:E146-E162.
18. Wei Z, Lei X, Petersen PS, Aja S, Wong GW. Targeted deletion of C1q/TNF-related protein 9 increases food intake, decreases insulin sensitivity, and promotes hepatic steatosis in mice. *Am J Physiol Endocrinol Metab*. 2014;306:E779-E790.
19. Wei Z, Peterson JM, Lei X, et al. C1q/TNF-related protein-12 (CTRP12), a novel adipokine that improves insulin sensitivity and glycemic control in mouse models of obesity and diabetes. *J Biol Chem*. 2012;287:10301-10315.
20. Byerly MS, Petersen PS, Ramamurthy S, et al. C1q/TNF-related Protein 4 (CTRP4) is a unique secreted protein with two tandem C1q domains that functions in the hypothalamus to modulate food intake and body weight. *J Biol Chem*. 2014;289:4055-4069.
21. Byerly MS, Swanson R, Wei Z, Seldin MM, McCulloh PS, Wong GW. A central role for C1q/TNF-related protein 13 (CTRP13) in modulating food intake and body weight. *PLoS One*. 2013;8:e62862.
22. Peterson JM, Aja S, Wei Z, Wong GW. C1q/TNF-related protein-1 (CTRP1) enhances fatty acid oxidation via AMPK activation and ACC inhibition. *J Biol Chem*. 2012;287:1576-1587.
23. Peterson JM, Seldin MM, Wei Z, Aja S, Wong GW. CTRP3 attenuates diet-induced hepatic steatosis by regulating triglyceride metabolism. *Am J Physiol Gastrointest Liver Physiol*. 2013;305:G214-G224.
24. Peterson JM, Wei Z, Seldin MM, Byerly MS, Aja S, Wong GW. CTRP9 transgenic mice are protected from diet-induced obesity and metabolic dysfunction. *Am J Physiol Regul Integr Comp Physiol*. 2013;305:R522-R533.
25. Peterson JM, Wei Z, Wong GW. C1q/TNF-related protein-3 (CTRP3), a novel adipokine that regulates hepatic glucose output. *J Biol Chem*. 2010;285:39691-39701.
26. Seldin MM, Lei X, Tan SY, Stanson KP, Wei Z, Wong GW. Skeletal muscle-derived myonectin activates the mTOR pathway to suppress autophagy in liver. *J Biol Chem*. 2013;289:36073-36082.
27. Lahav R, Haim Y, Bhandarkar NS, et al. CTRP6 rapidly responds to acute nutritional changes, regulating adipose tissue expansion and inflammation in mice. *Am J Physiol Endocrinol Metab*. 2021;321:E702-E713.
28. Appari M, Breitbart A, Brandes F, et al. C1q-TNF-related protein-9 promotes cardiac hypertrophy and failure. *Circ Res*. 2017;120:66-77.

29. Uemura Y, Shibata R, Ohashi K, et al. Adipose-derived factor CTRP9 attenuates vascular smooth muscle cell proliferation and neointimal formation. *FASEB J*. 2013;27:25-33.
30. Zuo A, Zhao X, Li T, et al. CTRP9 knockout exaggerates lipotoxicity in cardiac myocytes and high-fat diet-induced cardiac hypertrophy through inhibiting the LKB1/AMPK pathway. *J Cell Mol Med*. 2020;24:2635-2647.
31. Zheng Q, Yuan Y, Yi W, et al. C1q/TNF-related proteins, a family of novel adipokines, induce vascular relaxation through the adiponectin receptor-1/AMPK/eNOS/nitric oxide signaling pathway. *Arterioscler Thromb Vasc Biol*. 2011;31:2616-2623.
32. Kambara T, Ohashi K, Shibata R, et al. CTRP9 protein protects against myocardial injury following ischemia-reperfusion through AMP-activated protein kinase (AMPK)-dependent mechanism. *J Biol Chem*. 2012;287:18965-18973.
33. Li Y, Wang W, Chao Y, Zhang F, Wang C. CTRP13 attenuates vascular calcification by regulating Runx2. *FASEB J*. 2019;33:9627-9637.
34. Yan W, Guo Y, Tao L, et al. C1q/tumor necrosis factor-related protein-9 regulates the fate of implanted mesenchymal stem cells and mobilizes their protective effects against ischemic heart injury via multiple novel signaling pathways. *Circulation*. 2017;136:2162-2177.
35. Rodriguez S, Little HC, Daneshpajouhnejad P, et al. Aging and chronic high-fat feeding negatively affect kidney size, function, and gene expression in CTRP1-deficient mice. *Am J Physiol Regul Integr Comp Physiol*. 2021;320:R19-R35.
36. Rodriguez S, Little HC, Daneshpajouhnejad P, et al. Late-onset renal hypertrophy and dysfunction in mice lacking CTRP1. *FASEB J*. 2020;34:2657-2676.
37. Han S, Jeong AL, Lee S, et al. C1q/TNF-alpha–related protein 1 (CTRP1) maintains blood pressure under dehydration conditions. *Circ Res*. 2018;123:e5-e19.
38. Hamoud N, Tran V, Aimi T, et al. Spatiotemporal regulation of the GPCR activity of BAI3 by C1qL4 and Stabilin-2 controls myoblast fusion. *Nat Commun*. 2018;9:4470.
39. Cho Y, Kim HS, Kang D, et al. CTRP3 exacerbates tendinopathy by dysregulating tendon stem cell differentiation and altering extracellular matrix composition. *Sci Adv*. 2021;7:eabg6069.
40. Youngstrom DW, Zondervan RL, Doucet NR, et al. CTRP3 regulates endochondral ossification and bone remodeling during fracture healing. *J Orthop Res*. 2020;38:996-1006.
41. Schaffler A, Buechler C. CTRP family: linking immunity to metabolism. *Trends Endocrinol Metab*. 2012;23:194-204.
42. Kopp A, Bala M, Buechler C, et al. C1q/TNF-related protein-3 represents a novel and endogenous lipopolysaccharide antagonist of the adipose tissue. *Endocrinology*. 2010;151:5267-5278.
43. Murayama MA, Kakuta S, Inoue A, et al. CTRP6 is an endogenous complement regulator that can effectively treat induced arthritis. *Nat Commun*. 2015;6:8483.
44. Murayama MA, Chi HH, Matsuoka M, Ono T, Iwakura Y. The CTRP3-AdipoR2 axis regulates the development of experimental autoimmune encephalomyelitis by suppressing Th17 cell differentiation. *Front Immunol*. 2021;12:607346.
45. Yuzaki M. Synapse formation and maintenance by C1q family proteins: a new class of secreted synapse organizers. *Eur J Neurosci*. 2010;32:191-197.
46. Martinelli DC, Chew KS, Rohlmann A, et al. Expression of C1ql3 in discrete neuronal populations controls efferent synapse numbers and diverse behaviors. *Neuron*. 2016;91:1034-1051.
47. Kakegawa W, Mitakidis N, Miura E, et al. Anterograde C1ql1 signaling is required in order to determine and maintain a single-winner climbing fiber in the mouse cerebellum. *Neuron*. 2015;85:316-329.
48. Sigoillot SM, Iyer K, Binda F, et al. The secreted protein C1QL1 and its receptor BAI3 Control the synaptic connectivity of excitatory inputs converging on cerebellar Purkinje cells. *Cell Rep*. 2015;10:820-832.
49. Wei Z, Seldin MM, Natarajan N, Djemal DC, Peterson JM, Wong GW. C1q/Tumor necrosis factor-related protein 11 (CTRP11), a novel adipose stroma-derived regulator of adipogenesis. *J Biol Chem*. 2013;288:10214-10229.
50. Tan A, Ke S, Chen Y, et al. Expression patterns of C1ql4 and its cell-adhesion GPCR Bai3 in the murine testis and functional roles in steroidogenesis. *FASEB J*. 2019;33:4893-4906.
51. Liu F, Tan A, Yang R, et al. C1ql1/Ctrp14 and C1ql4/Ctrp11 promote angiogenesis of endothelial cells through activation of ERK1/2 signal pathway. *Mol Cell Biochem*. 2017;424:57-67.
52. Bolliger MF, Martinelli DC, Sudhof TC. The cell-adhesion G protein-coupled receptor BAI3 is a high-affinity receptor for C1q-like proteins. *Proc Natl Acad Sci U S A*. 2011;108:2534-2539.
53. Rodriguez S, Stewart AN, Lei X, et al. PRADC1: a novel metabolic-responsive secretory protein that modulates physical activity and adiposity. *FASEB J*. 2019;33:14748-14759.
54. Zheng H, Shin AC, Lenard NR, et al. Meal patterns, satiety, and food choice in a rat model of Roux-en-Y gastric bypass surgery. *Am J Physiol Regul Integr Comp Physiol*. 2009;297:R1273-R1282.
55. Sarver DC, Xu C, Cheng Y, Terrillion CE, Wong GW. CTRP4 ablation impairs associative learning and memory. *FASEB J*. 2021;35:e21910.
56. Schneider CA, Rasband WS, Eliceiri KW. NIH Image to ImageJ: 25 years of image analysis. *Nat Methods*. 2012;9:671-675.
57. Schmittgen TD, Livak KJ. Analyzing real-time PCR data by the comparative C(T) method. *Nat Protoc*. 2008;3:1101-1108.
58. Weisberg SP, McCann D, Desai M, Rosenbaum M, Leibel RL, Ferrante AW Jr. Obesity is associated with macrophage accumulation in adipose tissue. *J Clin Invest*. 2003;112:1796-1808.
59. Sun K, Tordjman J, Clement K, Scherer PE. Fibrosis and adipose tissue dysfunction. *Cell Metab*. 2013;18:470-477.
60. Masschelin PM, Cox AR, Chernis N, Hartig SM. The impact of oxidative stress on adipose tissue energy balance. *Front Physiol*. 2019;10:1638.
61. Mathis D. Immunological goings-on in visceral adipose tissue. *Cell Metab*. 2013;17:851-859.
62. Hotamisligil GS. Inflammation and metabolic disorders. *Nature*. 2006;444:860-867.
63. Birsoy K, Chen Z, Friedman J. Transcriptional regulation of adipogenesis by KLF4. *Cell Metab*. 2008;7:339-347.
64. Chen Z, Torrens JI, Anand A, Spiegelman BM, Friedman JM. Krox20 stimulates adipogenesis via C/EBPbeta-dependent and -independent mechanisms. *Cell Metab*. 2005;1:93-106.
65. Park YK, Ge K. Glucocorticoid receptor accelerates, but is dispensable for, adipogenesis. *Mol Cell Biol*. 2017;37:e00260-00216.
66. Park YK, Wang L, Giampietro A, Lai B, Lee JE, Ge K. Distinct roles of transcription factors KLF4, Krox20, and peroxisome

proliferator-activated receptor gamma in adipogenesis. *Mol Cell Biol*. 2017;37:e00554-00516.
67. Goodpaster BH, Sparks LM. Metabolic flexibility in health and disease. *Cell Metab*. 2017;25:1027-1036.
68. Wolf RM, Lei X, Yang ZC, Nyandjo M, Tan SY, Wong GW. CTRP3 deficiency reduces liver size and alters IL-6 and TGFbeta levels in obese mice. *Am J Physiol Endocrinol Metab*. 2016;310:E332-E345.
69. Mauvais-Jarvis F, Arnold AP, Reue K. A Guide for the design of pre-clinical studies on sex differences in metabolism. *Cell Metab*. 2017;25:1216-1230.
70. Miller LR, Marks C, Becker JB, et al. Considering sex as a biological variable in preclinical research. *FASEB J*. 2017;31:29-34.
71. Mauvais-Jarvis F. Sex differences in metabolic homeostasis, diabetes, and obesity. *Biol Sex Differ*. 2015;6:14.
72. Kelly DM, Jones TH. Testosterone: a metabolic hormone in health and disease. *J Endocrinol*. 2013;217:R25-R45.
73. Zurlo F, Larson K, Bogardus C, Ravussin E. Skeletal muscle metabolism is a major determinant of resting energy expenditure. *J Clin Invest*. 1990;86:1423-1427.
74. Park S, Shimada K, Fujihara Y, et al. CRISPR/Cas9-mediated genome-edited mice reveal 10 testis-enriched genes are dispensable for male fecundity. *Biol Reprod*. 2020;103:195-204.
75. Miyata H, Castaneda JM, Fujihara Y, et al. Genome engineering uncovers 54 evolutionarily conserved and testis-enriched genes that are not required for male fertility in mice. *Proc Natl Acad Sci U S A*. 2016;113:7704-7710.
76. Noda T, Sakurai N, Nozawa K, et al. Nine genes abundantly expressed in the epididymis are not essential for male fecundity in mice. *Andrology*. 2019;7:644-653.
77. Xia JY, Sun K, Hepler C, et al. Acute loss of adipose tissue-derived adiponectin triggers immediate metabolic deterioration in mice. *Diabetologia*. 2018;61:932-941.

SUPPORTING INFORMATION

Additional supporting information may be found in the online version of the article at the publisher's website.

How to cite this article: Sarver DC, Xu C, Carreno D, et al. CTRP11 contributes modestly to systemic metabolism and energy balance. *FASEB J*. 2022;36:e22347. doi:10.1096/fj.202200189RR